Eur. Phys. J. B **23**, 179–182 (2001)

THE EUROPEAN PHYSICAL JOURNAL B

EDP Sciences

Infrared transmission study of Pr_2CuO_4 crystal-field excitations

G. Riou[1,a], S. Jandl[1], M. Poirier[1], V. Nekvasil[2], M. Diviš[3], P. Fournier[1,4], R.L. Greene[4], D.I. Zhigunov[5], and S.N. Barilo[5]

[1] Centre de recherche sur les propriétés électroniques des matériaux avancés, Département de Physique, Université de Sherbrooke, Sherbrooke, J1K 2R1, Canada
[2] Institute of Physics, Czech Academy of Sciences, Cukrovarnická 10, 162 53 Praha 6, Czech Republic
[3] Department of electron systems, Charles University, Ke Karlovu 2, 121 16 Praha 2, Czech Republic
[4] Center for Superconductivity Research, Dept. of Physics, University of Maryland, College Park, MD 20742, USA
[5] Institute of Solids State and Semiconductors Physics, National Academy of Science, 17 P. Brovka street, Minsk 220072, Belarus

Received 25 April 2001

Abstract. We present an infrared crystal-field study of Pr_2CuO_4 single crystals and thin films. Excitations from the ground state multiplet $^3H_4$ to the $^3H_5$, $^3H_6$, $^3F_2$ and $^3F_3$ excited multiplets are observed in both single crystals and thin films. A precise set of crystal-field parameters, that reproduces the energy and the symmetry of the levels, is determined.

PACS. 74.25.Gz Optical properties – 71.70.Ch Crystal and ligand fields – 74.72.Jt Other cuprates

1 Introduction

The local probe that constitute the rare earth crystal field excitations has been successfully used to study local physical properties [1]. Particularly, Raman scattering and infrared spectroscopy have proven to be useful techniques in the determination of rare earth crystal field (CF) levels in the electron doped cuprates $Re_{2-x}Ce_xCuO_4$ [2,3] and more recently in the hole doped cuprates $Re_{1+x}Ba_{2-x}Cu_3O_6$ [4], providing additional information on the electronic and magnetic properties of the cuprate compounds.

Pr^{3+} CF excitations in Pr_2CuO_4 and $Pr_{2-x}Ce_xCuO_4$ have been observed by Raman [2,5] and neutron scattering [6]. In addition to the regular site, inequivalent Pr^{3+} sites of lower symmetry have been reported. Such inequivalent sites were assumed to be a characteristic structural instability of the 2-1-4 compounds, also responsible for the $\approx$580 cm^{-1} local phonon mode detected by Raman scattering [7].

In order to further refine our understanding of the CF in the mother compound, using it as a template for $Pr_{2-x}Ce_xCuO_4$, we present an infrared transmission study of Pr_2CuO_4 single crystals and thin films. The objectives are: (i) to complete the former (CF) Raman scattering studies of single crystals [5], (ii) to improve the determination of CF parameters that essentially depends on the symmetry and the number of the detected transitions, (iii) to determine thin films crystallite orientation and defects.

[a] e-mail: griou@physique.usherb.ca

2 Experiment

Infrared transmission spectra of Pr_2CuO_4 single crystals and thin films have been recorded as a function of temperature. The single crystals were grown by top-seeded solution method [8] and polished down to 25 μm along the z-axis. The thin films were obtained by pulsed-laser deposition [9] with an average thickness of 3000 Å. A complementary Raman scattering study enabled to check the orientation of the Pr_2CuO_4 samples, prior to the infrared measurements, as well as to study low energy phonons. The samples were mounted in a continuous-flow temperature regulated helium cryostat and 1 cm^{-1} resolution transmission spectra were obtained in the 1800–8000 cm^{-1} energy range using a Fourier-transform interferometer (BOMEM DA3.002) equipped with a quartz source, an InSb detector and a CaF_2 beam splitter.

In order to further characterize the Pr_2CuO_4 single crystals, microwave conductivity at 16.5 GHz was measured, in the 4.2–300 K temperature range, using the standard cavity perturbation technique [10]. This contactless technique is well suited for the measurements of electrical conductivity in anisotropic materials [11].

3 Results and discussion

The sample orientation was determined by Raman scattering. For the Pr_2CuO_4 single crystal, A_{1g} phonon and $A^\star$ local mode were observed in the zz configuration around 228 cm^{-1} and 571 cm^{-1} respectively (Fig. 1). Even

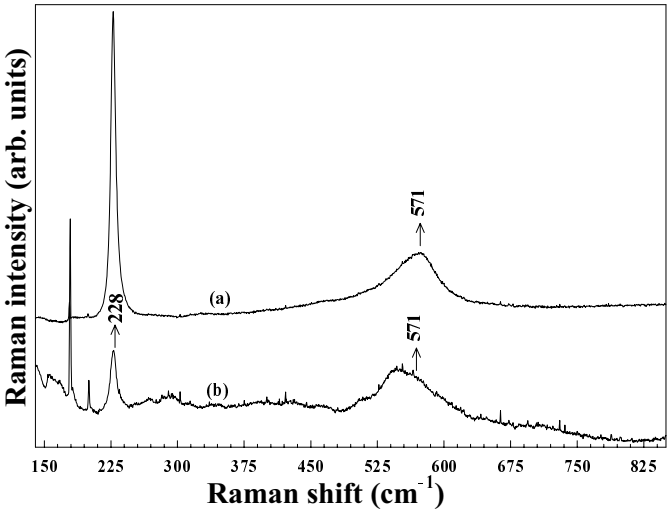

Fig. 1. Room temperature Raman-active excitations of a Pr_2CuO_4 single crystal in the $x(zz)\overline{x}$ configuration (a) and a Pr_2CuO_4 thin film in the $z(xy)\overline{z}$ configuration (b).

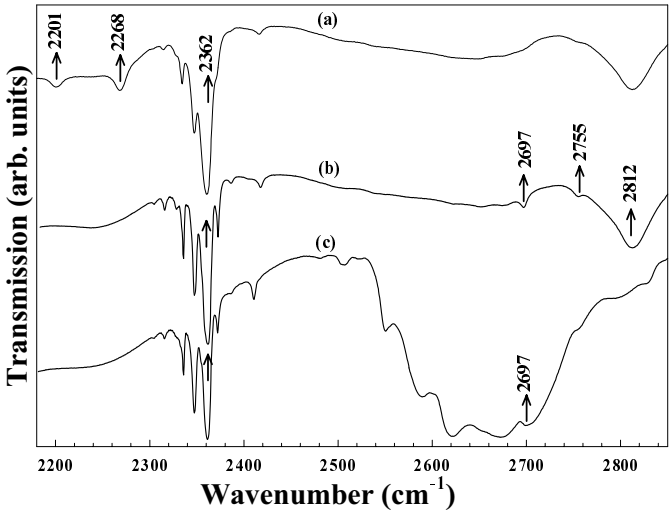

Fig. 2. Pr_2CuO_4 single crystal transmission for $\mathbf{E} \perp \mathbf{Z}$ at 77 K (a) and 20 K (b), and for $\mathbf{E} \parallel \mathbf{Z}$ at 20 K (c).

though, the A* local mode is symmetry forbidden in the thin film xy-plane, its detection, as shown in Figure 1, indicates some crystallite mis-orientation, in agreement with previous analysis of the X-ray diffraction pattern [9].

The C_{4v} Pr^{3+} site symmetry causes the lifting of the free ion $4f^2$ state multiplets degeneracy according to the representations of Table 1 (column 2). Assuming a perfect orientation of the crystal, $\Gamma_3 \rightarrow \Gamma_3$ and $\Gamma_5 \rightarrow \Gamma_5$ transitions are observed for $\mathbf{E} \parallel \mathbf{Z}$ while $\Gamma_5 \rightarrow \Gamma_1$, Γ_2, Γ_3 and Γ_4 transitions are observed for $\mathbf{E} \perp \mathbf{Z}$. These selection rules are used in the following section to identify the symmetry of the transitions.

In Figure 2, $^3H_4 \rightarrow {}^3H_5$ absorption bands at 2362 cm^{-1} (a), (b) and (c), 2755 cm^{-1} (b) and 2812 cm^{-1} (b) are associated with $\Gamma_3 \rightarrow \Gamma_5$ transitions while the absorption band at 2697 cm^{-1} (b) and (c) corresponds to a $\Gamma_3 \rightarrow \Gamma_3$ transition. Due to local distortions, selection rules are not rigorously respected in the case of the 2362 cm^{-1} (c) and 2697 cm^{-1} (b) bands. In order to pinpoint the exact energy positions of the transitions corresponding to the regular site, we have compared Pr_2CuO_4 absorption spectra to $Pr_{1.85}Ce_{0.15}CuO_4$ Raman CF excitations in which excitations due to defects have been identified. The nature of these defects could originate for example from local distortions and oxygen non-stoichiometry that would provoke, among other effects, the broadening of the 2697 cm^{-1} absorption band in (c). Absorption bands at 2201 and 2268 cm^{-1} are associated with transitions from the thermally populated 154 cm^{-1} Γ_5 [5] first excited level to Γ_4 ($2201 + 154 = 2355$ cm^{-1}) and Γ_2 ($2268 + 154 = 2422$ cm^{-1}) levels respectively.

In Figure 3 (b, c), $^3H_4 \rightarrow {}^3H_6$ absorption bands around 4416 cm^{-1}, 4610 cm^{-1} and 4990 cm^{-1} are associated with $\Gamma_3 \rightarrow \Gamma_5$ transitions, while the absorption band at 4921 cm^{-1} clearly observed in (a) (thin film) saturates in (d) (single crystal). It is associated with a $\Gamma_3 \rightarrow \Gamma_3$ transition. The observation of such a transition in thin films helps us to determine its exact energy value. It is essentially a consequence of a few percent mis-oriented crystallites as reported by Maiser *et al.* [9] and as confirmed by Raman scattering measurements (Fig. 1). The absorption band detected at 4343 cm^{-1} (d) is associated with a $\Gamma_3 \rightarrow \Gamma_3$ transition. Absorption bands at 4189, 4262 and 4767 cm^{-1} (Fig. 3b) are associated with transitions from the thermally populated 154 cm^{-1} Γ_5 [5] first excited level to Γ_3 ($4189 + 154 = 4343$ cm^{-1}), Γ_5 ($4262 + 154 = 4416$ cm^{-1}) and Γ_3 ($4767 + 154 = 4921$ cm^{-1}) levels respectively.

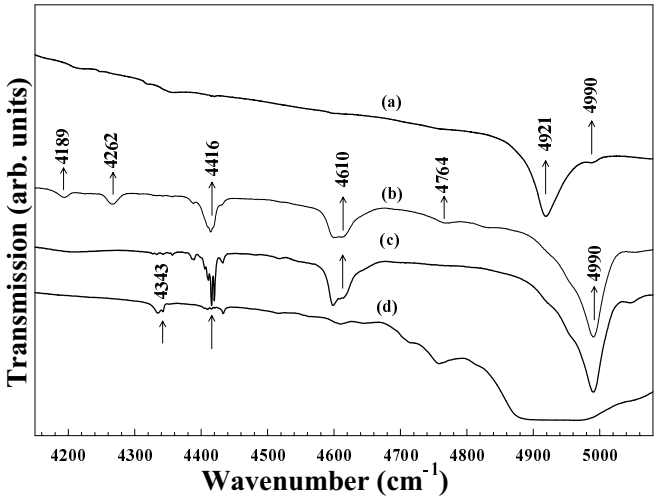

Fig. 3. Pr_2CuO_4 thin film transmission for $\mathbf{E} \perp \mathbf{Z}$ at 20 K (a), Pr_2CuO_4 single crystal transmission for $\mathbf{E} \perp \mathbf{Z}$ at 100 K (b) and 20 K (c) and for $\mathbf{E} \parallel \mathbf{Z}$ at 20 K (c).

In Figure 4, $^3H_4 \rightarrow {}^3F_2$ and $^3H_4 \rightarrow {}^3F_3$ absorption bands at (5432 cm^{-1}, 6828 cm^{-1}) and (5398 cm^{-1}, 6550 cm^{-1}) correspond to $\Gamma_3 \rightarrow \Gamma_5$ and $\Gamma_3 \rightarrow \Gamma_3$ transitions respectively. High temperature absorption bands at (5328 cm^{-1}, 5295 cm^{-1}) and (6417 cm^{-1}, 6674 cm^{-1}) are associated with transitions from the thermally populated

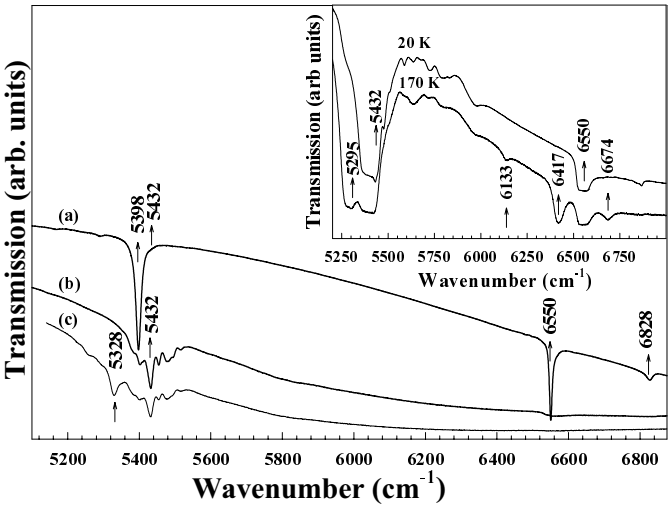

Fig. 4. Pr_2CuO_4 thin film transmission for $\mathbf{E} \perp \mathbf{Z}$ at 20 K (a) and single crystal transmission for $\mathbf{E} \perp \mathbf{Z}$ at 20 K (b) and 77 K (c). Inset: Pr_2CuO_4 single crystal temperature evolution of the Pr^{3+} $^3F_2$ and $^3F_3$ CF absorption bands for $\mathbf{E} \parallel \mathbf{Z}$.

154 cm^{-1} Γ_5 level to Γ_4, Γ_1, Γ_5 levels respectively. The transition from the ground state multiplet 695 cm^{-1} Γ_5 level to the 6828 cm^{-1} Γ_5 level corresponds to the absorption band at 6133 cm^{-1}. Table 1 summarizes our results together with previous measurements by CF Raman scattering.

We analyze the data by using the following CF Hamiltonian written with one-electron irreducible tensor operators:

$$H_{\mathrm{CF}} = \sum_{k,q} B_{kq} C_q^k \qquad (1)$$

where C_q^k is the qth component of a spherical tensor operator of rank k, and B_{kq} is the corresponding CF parameter. The C_{4v} symmetry of the Pr^{3+} site implies that only five CF parameters (B_{20}, B_{40}, B_{44}, B_{60}, B_{64}) are nonzero. In our calculations, we have diagonalized the matrix of the operator H_{CF} (Eq. (1)) within a truncated basis set which includes the 7 lowest J multiplets, considering the free ion intermediate coupling wave functions and energies [12]. In Table 2, our best-fit CF parameters are compared with previous results. A relatively good agreement is obtained with the CF parameters as determined by Raman scattering [5]. Also the theoretical value $B_{20} = -174$ cm^{-1}, which we obtained using the density functional theory based method [4], compares reasonably well with our best-fit value given in the last column in Table 2. The measured CF excitations are compared with our fit in Table 1. The good precision of the fit achieved is characterized by a mean error of ≈8.5 cm^{-1}.

The presence of additional absorption bands could be attributed to inequivalent Pr^{3+} sites due to oxygen non-stoichiometry or lattice distortions as previously reported by neutron and Raman studies of $Pr_{2-x}Ce_xCuO_4$ and $Nd_{2-x}Ce_xCuO_4$ [1,5]. In order to verify the presence of such defects, we have measured the in-plane temperature

Table 1. Pr^{3+} ion CF levels (in cm^{-1}) in Pr_2CuO_4 as observed experimentally and predicted by the CF parameters. Note that $^2F_3$ and $^2F_4$ multiplets overlap.

J	$i(\Gamma_i)$	Experiment		Theory	
		Ref. [5]	This work	Ref. [5]	This work
$^3H_4$	3	0	0	−3	4
	5	154	154	154	147
	1			670	637
	4			684	692
	5	695	695	696	697
	2			721	744
	1			751	775
$^3H_5$	4		2355	2360	2354
	5	2363	2362	2367	2362
	2		2422	2420	2417
	1			2523	2532
	3	2696	2697	2697	2694
	5	2772	2755	2767	2754
	2			2769	2765
	5		2812	2803	2821
$^3H_6$	3	4343	4343	4343	4351
	1			4403	4405
	5	4416	4416	4416	4419
	2			4561	4597
	5		4610	4624	4619
	4			4899	4902
	3	4928	4921	4929	4909
	5	5004	4990	5004	4977
	1			4983	4985
	4			5062	5055
$^3F_2$	3		5398		5397
	5		5432		5438
	1		5449		5451
	4		5482		5479
$^3F_3$	3		6550		6553
	5		6571		6568
	5		6828		6830
	2				6832
	4				7026
$^3F_4$	5				6998
	1				7041
	3				7095
	4				7186
	2				7212
	5				7246
	1				7349

Table 2. Pr^{3+} ion CF parameters (in cm^{-1}). Given in brackets are the mean errors associated with the fitting parameters.

CF parameters	Ref. [5]	This work
B_{20}	−235 (13)	−294 (15)
B_{40}	−2287 (29)	−2302 (50)
B_{44}	1864 (14)	1910 (24)
B_{60}	32 (32)	147 (37)
B_{64}	1519(19)	1469 (42)

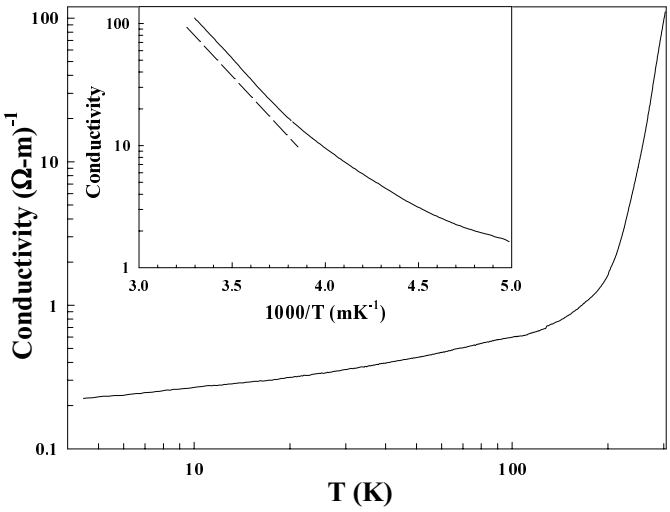

Fig. 5. Pr_2CuO_4 single crystal microwave conductivity at 16.5 GHZ as a function of temperature on a log-log scale. Inset: Microwave conductivity (log scale) as a function of the inverse of temperature for $T \geq 250$ K.

dependence microwave conductivity of a Pr_2CuO_4 single crystal extracted from the same batch as the ones studied in infrared transmission (Fig. 5). The temperature evolution of the microwave conductivity mimics a semiconducting character above 150 K following the functional form $\exp(-E_a/k_BT)$ with $E_a = 0.32$ eV. Below 150 K, the carriers are frozen on impurity sites and only hopping conductivity regime remains possible. Such observation is compatible with the optical conductivity of Pr_2CuO_4 that reveals the existence of in-gap states associated with oxygen vacancies [13]. Thus some of the additional absorption bands, detected by our infrared transmission measurements, could be attributed to oxygen related defects.

4 Conclusion

We have reported the first Pr^{3+} CF infrared absorption study in Pr_2CuO_4. 21 CF levels of the five first excited multiplets have been observed. In addition to the C_{4v} symmetry regular site, non-regular sites for Pr^{3+} have been detected in the single crystals. Measurements of the CF excitations in the thin films confirm the single crystal results. They also allow a precise determination of $\Gamma_3 \rightarrow \Gamma_3$ transitions associated with mis-oriented crystallites within the thin films. The calculation of the CF parameters provides a good fit of the observed Pr^{3+} CF levels and a better description of the microscopic interactions embedded in the CF Hamiltonian. An extension to this work, for a better understanding of the inhomogeneities and their effects, would be to study various contents of Cerium doped Pr_2CuO_4 in analogy with $Nd_{2-x}Ce_xCuO_4$ [3].

We thank J. Rousseau and M. Castonguay for technical assistance. S.J., P.F. and M.P. acknowledge support from the Natural Science and Engineering Research Council of Canada (NSERC) and le Fonds de Formation de Chercheurs et l'Aide à la Recherche (FCAR) du Gouvernement du Québec. P.F. acknowledges the support of the Canadian Institute of Advanced Research (CIAR). Also gratefully acknowledged is the Grant Agency of the Czech Republic for its grants No. 202/00/1602 and 202/99/184 (V.N., M.D.) and the Grant Agency of Charles University for its grant No. 145/2000/B-FYZ (M.D.). Work done in Maryland is supported by a DCMP NSF grant DMR 9732796.

References

1. P. Allenspach, A. Furrer, F. Fauth, M. Guillaume, W. Hengeler, J. Mesot, S. Rosenkranz, Physica B, **213-214**, 78 (1995).
2. S. Jandl, T. Strach, T. Ruf, M. Cardona, V. Nekvasil, D.I. Zhigunov, S.N. Barilo, S.V. Shiryaev, Physica C **322**, 87 (1999).
3. S. Jandl, P. Richard, M. Poirier, V. Nekvasil, A.A. Nugroho, A.A. Menovsky, D.I. Zhigunov, S.N Barilo, S.V. Shiryaev, Phys. Rev. B **61**, 12882 (2000).
4. D. Barba, S. Jandl, V. Nekvasil, M. Maryško, M. Diviš, A.A Martin, C.T. Lin, M. Cardona, T. Wolf, Phys. Rev. B **63**, 4528 (2001).
5. S. Jandl, T. Strach, T. Ruf, V. Nekvasil, M. Iliev, D.I. Zhigunov, S.N. Barilo, S.V. Shiryaev, Phys. Rev. B **56**, 5049 (1997).
6. C.-K. Loong, L. Soderholm, Phys. Rev. B **48**, 14001 (1993).
7. E.T. Heyen, R. Liu, M. Cardona, S. Pinol, R.J. Melville, D.McK. Paul, E. Moràn, M.A. Alario-Franco, Phys. Rev. B **43**, 2857 (1991).
8. J.L. Peng, Z.Y. Li, R.L. Greene, Physica C **177**, 79 (1991).
9. E. Maiser, P. Fournier, J.L. Peng, F.M. Araujo-Moreira, T. Venkatesan, R.L. Greene, G. Czjzek, Physica C **297**, 15 (1998).
10. L.I. Buranov, I.F. Schegolev, Prib. Tekh. Eksp. **2**, 171 (1971).
11. S. Jandl, P. Richard, J. Trottier, K. Frikach, M. Poirier, D.I. Zhigunov, S.N. Barilo, S.V. Shiryaev, Physica C **297**, 64 (1998).
12. E. Antic-Fidancev, J. Holsa, J.-C. Krupa, M. Lemaitre-Blaise, P. Porcher, J. Phys. Cond. Matt. **4**, 8321 (1992).
13. T. Arima, Y. Tokura, S. Uchida, Phys. Rev. B **48**, 6597 (1993).